Osteoarthritis and Cartilage (2003) **11,** 65–77

1063–4584/03/$30.00/0
doi:10.1053/joca.2002.0867

Osteoarthritis and Cartilage

International Cartilage Repair Society

OARSI OSTEOARTHRITIS RESEARCH SOCIETY INTERNATIONAL

Topographical analysis of the structural, biochemical and dynamic biomechanical properties of cartilage in an ovine model of osteoarthritis

R. C. Appleyard*, D. Burkhardt†, P. Ghosh†, R. Read‡, M. Cake‡, M. V. Swain§ and G. A. C. Murrell*

**Orthopaedic Research Institute, St George Hospital Campus (University of New South Wales), Kogarah, NSW, Australia; †Institute of Bone and Joint Research, Royal North Shore Hospital (University of Sydney), St Leonards, NSW, Australia; ‡Division of Veterinary and Biomedical Sciences, Murdoch University, Perth, WA, Australia; §Biomaterials Science Research Unit, Faculty of Dentistry, and Department of Mechanical Engineering (University of Sydney), NSW, Australia*

Summary

Objective: The relationship between the topographical variations in the structural, biochemical and dynamic biomechanical properties of articular cartilage (AC) before and 6 months after meniscectomy has not been previously reported but is clearly relevant to our understanding of the role of mechanical factors on the pathogenesis of osteoarthritis (OA). The objective of this study was to address this deficiency using an ovine model of OA induced by bilateral lateral meniscectomy.

Design: The dynamic effective shear modulus (G*) and phase lag were determined *ex vivo* at 26 individual locations over the medial and lateral tibial plateaux of non-operated and meniscectomized ovine joints 6 months after surgery using a novel hand-held dynamic indentation probe. AC thickness was measured with a needle penetration probe. The AC from the same topographical locations as indented was then analysed for sulfated glycosaminoglycans (S-GAG) as a measure of proteoglycan (PG) levels, collagen and water content. Histological evaluation of the collagen organization using quantitative analysis of birefringence intensity was performed on stained tissue sections from the same topographical locations of each animal.

Results: It was demonstrated that the AC of the entire lateral tibial compartment of the meniscectomized joints underwent significant local degenerative and compensatory changes as indicated by a decreased G* and an increase in phase lag and water content. This was accompanied by a decrease in PG content of the AC of the middle and inner regions. While the AC of the outer region of the lateral meniscectomized compartment showed a marked increase in PG content and a more than two-fold increase in thickness, these tissues were also found to be structurally inferior, as indicated by a decreased G* and abnormal collagen birefringence intensity. The AC thickness was elevated at all locations of the lateral and medial tibial plateau of the meniscectomized joints. Strong and significant correlations between the biomechanical and biochemical data were established for a number of the parameters examined, especially between collagen content and G*, collagen content and AC thickness, and G* and AC thickness. An inverse correlation between S-GAG content and G* was only apparent in non-operated control tissues, whereas correlations between collagen and water content, water content and G*, and water content and thickness were evident for AC of the meniscectomized tibial plateaux. Less striking changes were noted in the medial compartment where the intact meniscus remained in place. However, elevated PG content, thicker AC together with slight changes in G* suggested an early hypertrophic response in these tissues.

Conclusions: This study has highlighted the variable response of AC in different topographical regions of meniscectomized joints to the altered mechanical stresses introduced by this surgical procedure. The AC at the joint margins, while thicker and richer in PG, was found to be biomechanically softer (lower shear modulus) than normal AC, and because of this, would be expected to undergo degenerative changes with time leading to the onset of OA.

Key words: Articular cartilage, Meniscectomy, Biomechanics, Biochemistry.

Introduction

Total or partial excision of the knee joint menisci, due to symptoms arising from their failure as a result of degeneration or mechanical injury, is still a common orthopaedic procedure. However, this surgical intervention is frequently followed by premature degeneration of articular cartilage (AC) and the early onset of osteoarthritis (OA)[1–3]. This post-surgical sequela is considered to result from the imposition of high focal and shearing stresses on AC arising from the excision of the menisci, which have been shown to be important weight bearing and joint stabilizing structures[4–8].

Meniscectomy in adult sheep and other species reproduces the pathological changes in AC and subchondral bone which have been described for early OA in human joints. For this reason meniscectomized laboratory animals have been widely employed as models of OA and have provided valuable insights into the temporal changes which occur in AC and subchondral bone during the development and progression of this disorder[9].

Received 22 July 2002; revision accepted 18 October 2002.
Address correspondence to: A/Professor Peter Ghosh, Director, Institute of Bone and Joint Research, Level 5, University Clinic, Royal North Shore Hospital, St Leonards NSW 2065, Australia. Tel: +61 (2) 9926 7239; Fax: +61 (2) 9906 5368; E-mail: pghosh@mail.usyd.edu.au

Using the ovine model of lateral meniscectomy, it has been shown that in those regions adjacent to focal AC lesions, hypertrophy and osteophytosis occured[10]. Such hypertrophic changes in AC are considered to arise from an early response by chondrocytes to supraphysiological loading which may be followed at a later stage by a degenerative phase where the extracellular matrix is destroyed[11,12].

Previous experimental investigations which have sought to determine the influence of meniscectomy on the biomechanical and biochemical properties of AC have confined their examination to relatively few sites within the operated joint[12–14]. Our previous studies had clearly shown that significant changes in the composition and metabolism of AC takes place over the entire joint surface following meniscectomy[15–22]. The purpose of this investigation was therefore to build upon these earlier biomechanical and biochemical studies by mapping the entire tibial plateau, thereby gaining a better appreciation of the topographical variations that occur across a normal and degenerate joint.

We recently developed a hand-held indentation system, which was capable of accurately and rapidly measuring the dynamic biomechanical properties of AC[23]. The short time frame needed for measurements, using this instrument, would allow the collection of biomechanical data of AC from many joint locations without degradation, nor prejudice to its structural integrity. This device therefore offered the opportunity to generate meaningful topographical relationships between the biochemical and histological parameters and the biomechanical properties of AC in normal and meniscectomized joints.

In the present study we describe the results of a detailed topographical study of the composition and biomechanical properties of AC of the ovine tibial plateau before and 6 months after lateral meniscectomy. The data obtained revealed that the hypertrophic response in AC, which occurs adjacent to focal lesions and which was identified by increased AC thickness and PG content, was accompanied by a deterioration in its surface collagen assembly and biomechanical properties. We suggest that this early hypertrophic response by the cartilage matrix, which has hitherto been considered as a compensatory and protective process, may in fact render these tissues more susceptible to physical damage during weight-bearing activities.

Materials and methods

ANIMAL MODEL

Twelve aged (7-year-old) female pure-bred Merino sheep were used for this study. Six animals were subjected to open lateral meniscectomy (MEN) of both stifle joints as described previously[17], while the remaining six were used as non-operated controls (NOC). All animals were maintained under identical environmental conditions for 6 months, at which time they were sacrificed by intravenous infusion of phenobarbitone. The joints were opened and the tibial plateaux (including approximately 5 mm subchondral bone) were horizontally sectioned from the tibial long bone. These complete tibial osteochondral slabs were photographed, then wrapped in saline soaked gauze, sealed in plastic bags, and stored at −20°C. One left or right tibial plateau (alternately selected) from each animal was used for the conjoint biomechanical and biochemical studies, while the contralateral joint from the same animal was employed for the histological investigations. The protocol used for this study was approved by the animal ethics committee of Murdoch University (AEC 832R/00).

Fig. 1. Dynamic arthroscopic indentation device.

EXPERIMENTAL APPARATUS

The dynamic indentation device (Fig. 1) has been described previously[23]. Briefly, it incorporated a handle with a 120 mm long stainless steel tube (4 mm external diameter) extending from one end. Located at the end of the tube was a vibration unit that had a small non-porous cylindrical probe (0.5 mm diameter) attached, extending out of the side of the tube. A single frequency (20 Hz) sinusoidal waveform was applied to the device causing the probe to vibrate at equal frequency. The instrument was used to dynamically indent the AC by pressing the probe against the surface of the tissue with constant pressure (2.5 N). The system was connected to a computer, which provided graphical output of the biomechanical parameters. Dynamic stiffness and phase lag data were collected and saved each time a foot switch was activated.

BIOMECHANICAL ASSESSMENT

AC samples were removed from the freezer and placed in saline at room temperature for 1 h to thaw and equilibrate. The sample was then removed from the saline and a light grid was cast onto the exposed AC using a converted slide projector[19]. Using this grid as a guide, a standard 26-point array was marked on the AC surface of the lateral and medial tibial compartments with Picro Sirius red stain (Fig. 2). In-house experiments have shown that Picro Sirius stain had no effect on the biomechanical properties of AC and did not interfere with the subsequent biochemical analyses. Indentation tests were conducted sequentially at each marked location, repeated over three runs, and the average dynamic stiffness and phase lag of each location recorded. Surfaces that were not being assessed remained covered in saline soaked gauze to prevent dehydration. The entire indentation assessment of each tibial plateau was completed in less than 10 min. On completion of the indentation assessment, the thickness of the AC was determined using a needle penetration method similar to that previously described[24].

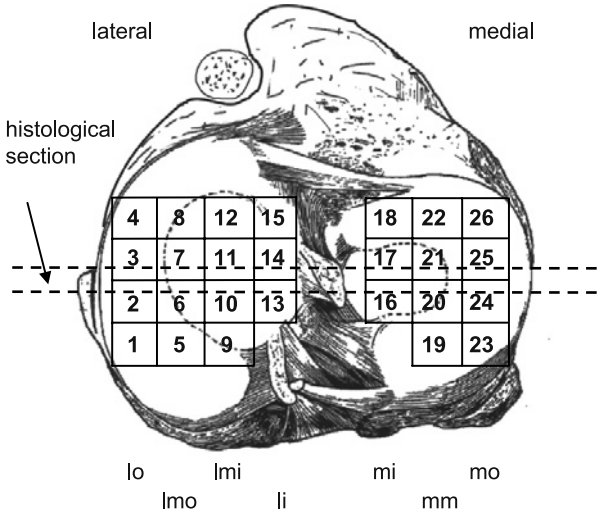

Fig. 2. Sites of indentation and biochemical analysis (N=26) across the lateral (l) (lo=outer, lmo=middle–outer, lmi=middle–inner, li=inner) and medial (m) (mi=inner, mm=middle, mo=outer) compartments of the tibial plateau. Full thickness medial-lateral histological sections were collected from the contralateral joint (dashed line).

The dynamic shear modulus (G*) was calculated using the theory published by Hayes *et al.*[25] where

$$G^* = \frac{dP^*}{dH^*}\frac{(1-\nu)}{4a\kappa}$$

and a is the indenter radius, dP^*/dH^* is the change in dynamic force divided by the change in dynamic displacement (dynamic stiffness), ν is the Poisson's ratio and κ is the theoretical correction function. Hayes *et al.*[25], tabulated the variation in κ with alteration in Poisson's ratio and aspect ratio, a/h, where h is the thickness of the AC beneath the indenter.

The effective shear modulus (G*) and phase lag are termed 'effective' because the biomechanical response is dependent on the frequency and boundary conditions of the test. However, it had been demonstrated that there was marginal change in these parameters[26,27] when AC was indented at frequencies above 4 Hz with the G* being of similar magnitude to the 'instantaneous' shear modulus generated during a step indentation test. As such, the Poisson's ratio was assumed to be 0.5.

BIOCHEMICAL ANALYSIS

Water content, PG content (as sulfated glycosaminoglycans (S-GAG)), and total collagen content (as hydroxyproline) were analysed using published methods. Briefly, 26 full depth squares of AC, corresponding to each indentation site (Fig. 2) were removed using a #11 scalpel blade. The water content was determined by weighing each sample before and after freeze-drying and was expressed in percent of the wet weight. The S-GAG content was assessed using a micro-adaptation of the dye binding assay originally described by Farndale *et al.*[28] but modified by us to analyse AC sections prepared for histology[20]. Each freeze-dried tissue sample, of known dry mass, was digested with papain (Sigma-Aldrich, Castle Hill NSW, Australia), and aliquots of this digest (in triplicate) mixed with 1,9-dimethylmethylene blue (Sigma-Aldrich, Castle Hill NSW, Australia), followed by measuring the absorbance in a plate reader at 650 nm. The S-GAG concentration was calculated from a standard curve using chondroitin-4-sulfate from bovine trachea (Sigma Chemical Co., Castle Hill NSW, Australia) as a standard. The collagen content was determined using a simplified microtiter plate adaptation of the hydroxyproline assay of Stegemann and Stalder[29]. Aliquots (200 μl) of the AC papain digests were vacuum dried and then hydrolysed in 250 μl of 6 N HCl for 16 h at 110°C. After addition of 250 μl 6 N NaOH to neutralize the HCl, the free hydroxyproline was oxidized to pyrrole with chloramine T (Sigma Chemical Co., Castle Hill NSW, Australia), the color developed by the addition of p-dimethylaminobenzaldehyde (Sigma Chemical Co., Castle Hill NSW, Australia) determined by absorption at 562 nm. The total hydroxyproline content was calculated from a standard curve using a hydroxyproline standard (Sigma Chemical Co., Castle Hill NSW, Australia) and, assuming that AC collagen contains 13.5% hydroxyproline, a factor of 7.4 was used to convert the hydroxy proline values to collagen.

HISTOLOGICAL ANALYSIS

Medial-lateral osteochondral slices (5 mm wide) were cut from tibial plateaux using a bandsaw according to the diagram shown in Fig. 2. Each section was fixed in 10% neutral buffered formalin, decalcified in 10% formic acid/5% formalin, dehydrated and double-embedded (methyl benzoate, celloidin, paraffin) such that full-depth cartilage/bone coronal sections were obtained. Sections for polarized light microscopy studies were treated with bovine testicular hyaluronidase (ICN Biomedicals, Australia) to remove PG, and were then stained with Picro Sirius red (PSR) in order to enhance observation of birefringence, using a modification of the method described by Junqueira *et al.*[30] and Arokoski *et al.*[31].

BIREFRINGENCE EVALUATION OF COLLAGEN ORGANIZATION

Quantitative analysis of birefringence intensity was conducted using methods similar to that described by Arokoski *et al.*[31]. Briefly, PSR-stained sections were viewed through a Leica DMLB polarization microscope (Leica, Germany) with a 5×/0.15 objective lens. Monochromatic light with a wavelength of 550 nm was achieved with an interference filter (Type: OG 550 nm, Schott, Germany) and used to transilluminate each specimen. With the superficial zone orientated at 45° to the lower polarization filter, full depth digital images (256 shades of grey, 700×570 pixel resolution) were collected using a digital camera (COHU 4910 series, COHU Pty Ltd, U.S.A.) and stored in TIFF format.

Images were collected of the lateral and medial (inner, middle and outer) regions of each histological section of each tibial plateau [Fig. 3 (left panel)]. A full thickness birefringence intensity profile of each image was generated using Image-Pro Plus analysis software (Media Cybernetics, U.S.A.). The width of the profile area was maintained at 150 pixels and its height determined by the full thickness of the uncalcified AC. The profile was then normalized by depth (0=cartilage surface, 1=calcified cartilage), and divided into 100 sub-zones to allow direct comparison between profiles of AC of varying thickness [Fig. 3 (right panel)].

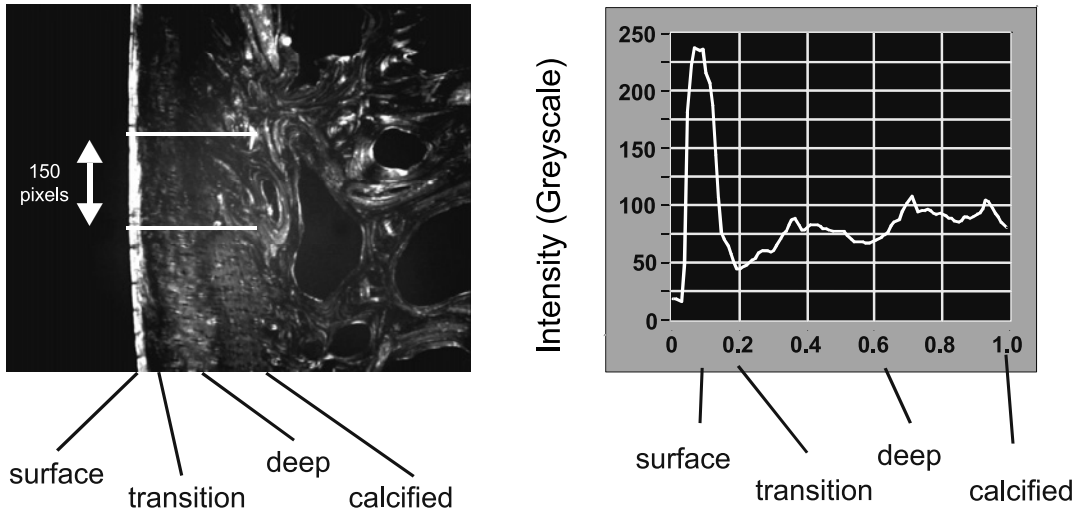

Fig. 3. Image of articular cartilage as viewed under polarized light (left panel) and its normalized birefringence intensity profile plot (right panel). The middle region of a lateral tibial plateau from a non-operated control joint is shown.

Table I

Summary table of the overall changes (in percent) in the biochemical and biomechanical properties of articular cartilage occurring in the lateral and medial tibial plateau within 6 months after lateral meniscectomy

	Lateral			Medial		
Collagen organization	↓		(P<0.01)	—		
Thickness (mm)	↑	58%	(P<0.0001)	↑	30%	(P<0.01)
G* (MPa)	↓	60%	(P<0.0001)	—		
Phase (degrees)	↑	17%	(P<0.05)	—		
Water content (%)	↑	5%	(P<0.001)	—		
Collagen content (μg/mg)	—	—	—	—		
Proteogylcan content (μg/mg)	↓	27%	(P<0.001)	—		

DATA PRESENTATION AND STATISTICAL ANALYSIS

The biochemical and biomechanical results generated by this study were represented as combined data maps consistent with each of the 26 topographical locations on the tibial plateau identified using the standard grid pattern employed to assign the individual sites (Fig. 2). Each cell entry represents the mean of six animals. A linear five-level colour scale graduation (lightest hue=lowest value; darkest hue=highest value) was used to illustrate the results (see Figs 5 and 7). The data from each location of each animal were also pooled into seven regions of interest, those being the inner (i), middle (m) and outer (o) regions of the lateral (l) and medial (m) compartments (lo, lmo, lmi, li, mi, mm and mo) (Fig. 2). These values represented the mean (N=6) of each region from the six animals used in each group and are shown as bar graphs (±1 S.D.) (see Figs 6 and 8). Overall biochemical, biomechanical and histological changes in the lateral and medial compartments of the NOC and MEN joints are represented in Table I. Significant differences between NOC and MEN were determined using the Student t-test.

Relationships between the measured parameters and between NOC and MEN were investigated using the Pearson correlation test. The combination of the six different parameters measured in this study provided for a total of 15 possible comparisons. (Table II). Each set was conducted for the entire tibial plateau (N=26; df=24; P<0.05 when r^2>0.15; P<0.01 when r^2>0.25), the lateral compartment only (N=15; df=13; P<0.05 when r^2>0.26; P<0.01 when r^2>0.41) the medial compartment only (N=11; df=9; P<0.05 when r^2>0.36; P<0.01 when r^2>0.55) and for the regions only (N=7; df=5; P<0.05 when r^2>0.56; P<0.01 when r^2>0.76).

Results

ANIMAL MODEL

The sheep meniscectomy model used in this study was characterized by the development of the morphological and histological changes in AC typical of early OA. In contrast, the NOC tibial plateaux AC exhibited a normal appearance with a smooth, glossy articular surface. The lateral compartment of the MEN joints all had a roughened AC surface, focal lesions and osteophyte formation on the outer margin consistent with previous observations[20–22], while the medial compartment appeared macroscopically normal (Fig. 4).

BIOMECHANICAL ASSESSMENT

The results of the biomechanical assessment are represented in Table I, Figs 5 and 6. The AC of the NOC joints had a significant variation in the thickness and G* (mean±1 S.D.) across the tibial plateau, ranging from a minimum thickness of 0.30±0.18 mm and maximum moduli of 2.67±1.92 MPa in the lateral–outer region (lo), to a

Table II

Summary of the correlations between five articular cartilage parameters analysed for the entire tibial plateau, the lateral tibial plateau, the medial tibial plateau and the seven designated regions of the tibial plateau of non-operated controls and meniscectomy groups

Parameter A	Parameter B	Entire tibial plateau (*N*=26; df=24)		Lateral tibial plateau (*N*=15; df=13)		Medial tibial plateau (*N*=11; df=9)		Regions (*N*=7; df=5)		Correlation	Comments
		NOC	MEN	NOC	MEN	NOC	MEN	NOC	MEN		
S-GAG	Collagen	0.01	0.01	0.01	0.05		0.05	0.01		Negative	Strong in lateral NOC
S-GAG	Shear modulus	0.01		0.01				0.01		Negative	NOC only
S-GAG	Thickness	0.01	0.05	0.01	0.05	0.05		0.05		Positive	Stronger in lateral NOC
Collagen	Moisture		0.01		0.05		0.05		0.01	Negative	MEN only
Collagen	Shear modulus	0.01	0.01	0.05	0.01	0.01	0.01		0.05	Positive	Slightly stronger in MEN
Collagen	Thickness	0.01	0.01	0.01	0.01	0.01	0.01	0.01	0.01	Negative	Very strong correlation
Moisture	Shear modulus	0.05	0.01		0.01		0.01		0.05	Negative	Strong correlation in MEN
Moisture	Thickness		0.01		0.01	0.05	0.01		0.01	Positive	Strong correlation in MEN
Shear modulus	Thickness	0.01	0.01	0.01	0.01	0.01	0.01	0.05	0.05	Negative	Strong correlation

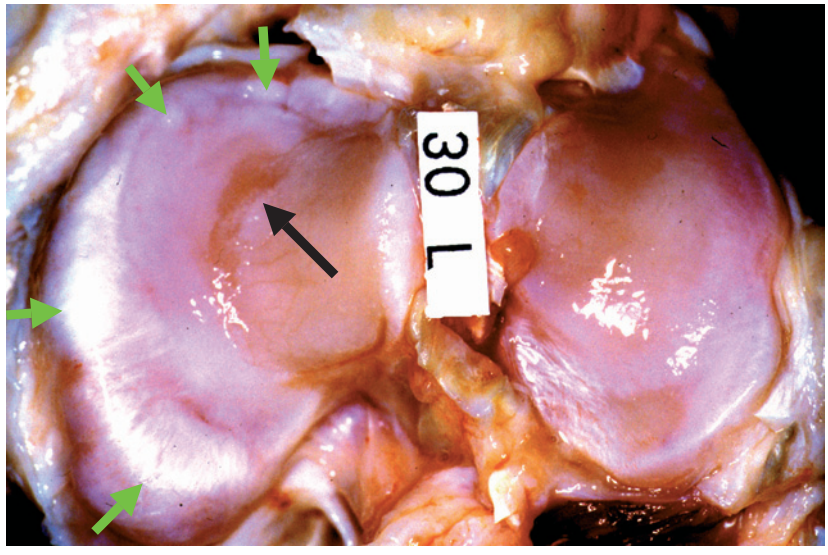

Fig. 4. Photograph of tibial plateau of a laterally meniscectomized joint showing articular cartilage lesions (black arrow) and osteophytosis at the joint margins (green arrows).

maximum thickness of 1.23±0.29 mm and minimum moduli of 0.19±0.12 MPa in the medial–inner region (mi). The phase lag was relatively constant (12.3±2.8°) across the entire plateau, although there was an increase (14.2±3.0°) at the medial–inner region (mi). MEN resulted in an overall increase in AC thickness across both the lateral (↑26–135%) and medial (↑19–30%) compartments. An overall decrease in G* (↓45–70%) was noted across the lateral tibial compartment, while the medial compartment remained unaffected. An increase in phase lag (↑15–18%) was evident on the lateral middle and inner (lmo, lmi, li) regions of the MEN tibial plateau. An increase in phase lag (↑11%) also occurred on the medial outer region of the MEN joints (Figs 5 and 6).

The most significant change in biomechanical and structural properties, as a result of MEN, occurred at the lateral–outer region (lo) where a 70% reduction in G* and 135% increase in AC thickness were observed. While the lateral–middle regions (lmo, lmi) of the MEN joint also demonstrated a significant decrease in G* (↓63–65%), the change in thickness (↑30–42%) was not as pronounced as that of the lateral–outer region (↑135%). This may be due to marginal erosion of the uncalcified AC in this high stress region of the MEN joints. There was, however, a significant increase in phase lag (↑15–18%) which would suggest an alteration in the viscoelastic response of the AC with the tissue becoming less elastic and more viscous.

It was interesting to note that AC of the inner and middle regions of the medial compartment (mi, mm), while of greater thickness (↑19–30%), showed no change in G* or phase lag resulting from the removal of the meniscus in the lateral compartment. There was, however, an increase in phase lag (↑11%) on the medial–outer region (mo) suggesting some modification of the tissue architecture. Possible reasons for this modification are addressed in the discussion.

BIOCHEMICAL COMPOSITION

The results of the biochemical analyses of AC are shown in Table I, Figs 7 and 8. MEN resulted in an increase in water content of the AC on the lateral middle and inner regions (lmi, li) when compared with the tissue of the NOC. The water content remained unchanged in the AC of the medial side of both groups, where the soft, uncovered medial–inner region (mi) showed the highest values overall.

A significant increase in PG content (↑52%) was measured in the lateral–outer region (lo) of the meniscectomized joints, while a significant decrease in PG content (↓21–32%) was found across the lateral middle and inner regions (lmo, lmi, li). There was also an unexpected, slight but consistent, increase in S-GAG content (↑14–19%) in the middle and outer regions (mm, mo) of the medial compartment (which remained protected by the meniscus) of the MEN group.

The total collagen content of the AC from both NOC and MEN groups was not significantly different from each other and was within a range of 39–60% (w/w) related to dry weight of the tissue. However, a gradual decrease was evident from about 60% in the outer lateral regions (lo, lmo) and 55% in the medial outer region (mo) to approximately 40% and 45% in the corresponding inner regions.

HISTOCHEMICAL/BIREFRINGENCE STUDIES

Significant alterations in the superficial collagen organization were observed as a result of meniscectomy as illustrated by Fig. 9. The most pronounced changes occurred at the lateral outer region where an almost complete loss of the superficial zone birefringence intensity peak was observed in the MEN joints, suggesting either a significant reduction in the collagen organization, or complete loss of the surface zone by erosion. A similar trend was noted in the lateral middle region.

Neither the lateral nor the medial compartments of the NOC and MEN joints had a superficial birefringence peak in the inner regions. This suggests that there was minimal collagen organization, even before meniscectomy, and may account for the roughened, velvet-like appearance and reduced biomechanical integrity of these regions.

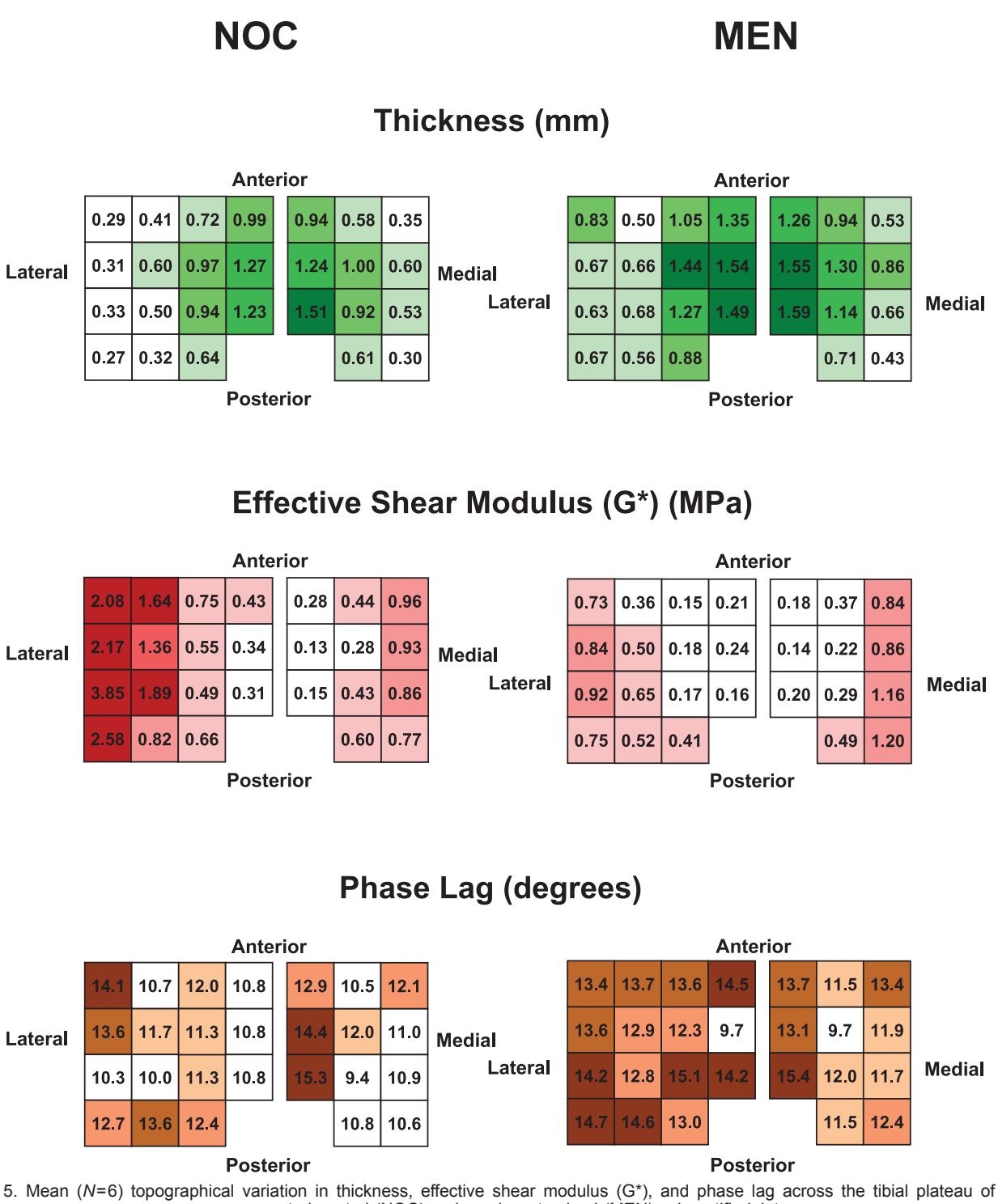

Fig. 5. Mean (N=6) topographical variation in thickness, effective shear modulus (G*), and phase lag across the tibial plateau of the non-operated control (NOC) and meniscectomized (MEN) ovine stifle joint.

There was no significant alteration in the deep zone birefringence in the lateral or medial, inner or middle regions as a result of meniscectomy. The lateral and medial outer regions both demonstrated an increase in deep zone birefringence, which may be due to collagen fibril reorganization.

BIOMECHANICAL AND BIOCHEMICAL CORRELATIONS

The three biochemical parameters (water, S-GAG and collagen content) and the three biomechanically measured parameters (G*, phase lag and thickness) were further analysed to determine what relationships existed between

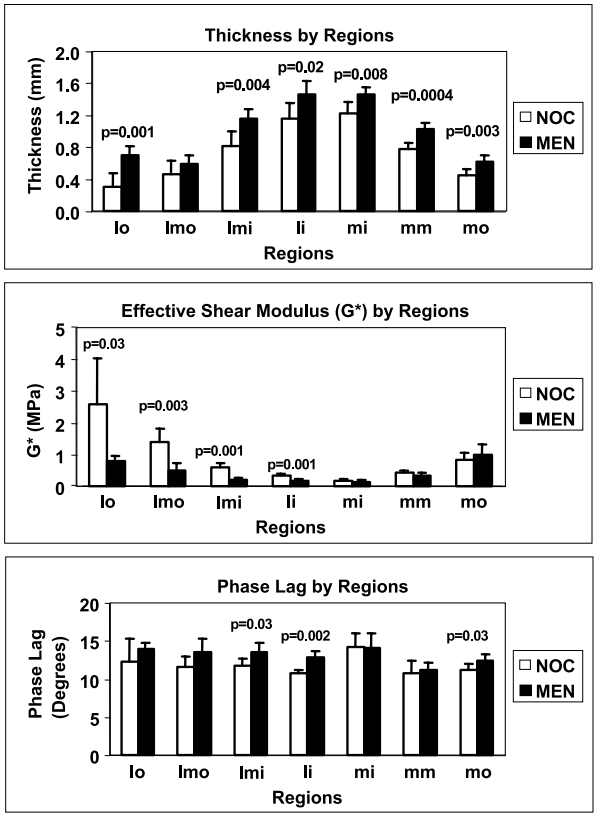

Fig. 6. Biomechanical properties [thickness, effective shear modulus (G*) and phase lag] of lateral and medial regions of tibial plateau articular cartilage of non-operated control (NOC) and meniscectomized (MEN) ovine stifle joints (N=6).

them. Table II summarizes the significant correlations identified between these parameters. As is evident, the strongest correlations were observed between collagen content and AC thickness [negative correlation (neg)] and between G* and thickness (neg), respectively, in both experimental groups. S-GAG and collagen content (neg), and S-GAG and thickness (pos) correlated well in the lateral compartment and when compared across the entire tibial plateau. These findings contrasted with the phase lag results, most of which did not correlate with any other parameter (not shown in Table II). The correlation between S-GAG and G* (neg) was only apparent in the NOC group, whereas strong correlations were noted only in the MEN group between water content and G* (neg), water content and thickness (pos), and water content and collagen content (neg), respectively.

Discussion

The results of the present study using the ovine model of OA have confirmed that 6 months after meniscectomy significant focal AC degeneration occurs across the lateral compartment as shown by a sharply decreased G*, slightly increased phase lag, a reduction in collagen organization, loss of PGs, and water content. Fewer, but none the less notable, alterations were observed in the medial compartment, which included an increase in thickness at every sample location, as well as increased S-GAG content and a slight increase in phase lag of AC at the middle and outer joint regions.

The most prominent change in AC thickness, G*, effective phase lag, PG content and collagen organization occurred within the middle and outer regions of the lateral tibial compartment, corresponding to areas which were previously protected by the lateral meniscus.

An overall increase in phase lag was detected in areas of high erosion on the lateral central plateau. This increase suggests that the tissue had become less elastic and more viscous (purely elastic response=0°, purely viscous response=90°). To our knowledge only two other studies have shown an increase in phase lag as a result of osteoarthritic cartilage degeneration[27,32]. Studies of PG in solution have demonstrated that in concentrated solutions the PG aggregates were dynamically stiffer and more elastic (lower phase lag) than solutions of the corresponding monomer subunits which exhibited a more viscous response[33,34]. The present findings are therefore consistent with the hypothesis that proteolytic degradation of PG, possibly in the G1-G2 inter-globular domain of the core protein, had occurred in the AC of the laterally MEN joints, resulting in a decreased G* and increased phase lag. While other studies have also shown that trypsin digestion of normal AC decreased its shear modulus and increased its phase lag[26,35], there is also a body of evidence suggesting that PG degradation does not affect the high loading rate or dynamic stiffness of AC[36–40]. We, like others[14,41,42], consider that the observed reduction in G* arising from meniscectomy, was more likely due to a disturbance in the AC collagen assembly and/or organization, with the contribution from the degradation of PG only playing a minor role. On the other hand, the increase in phase lag may be more dependent on the decrease in PG aggregation and the possible effects this may have on the structure of the collagen network. Furthermore, the negative correlation noted between water and total collagen content, which was only evident in the AC of the meniscectomized group, was consistent, by implication, with the findings of Bank *et al.*[43]. By quantitating the amount of degraded collagen in AC, this group presented experimental evidence to show that damage to the collagen network correlated with the extent of swelling of OA cartilage.

The lateral outer region (lo) of the meniscectomized joints demonstrated a significant increase in thickness and an increase in PG content relative to NOC, suggesting a hypertrophic response. However, the G* decreased sharply and the phase lag increased, indicating an abnormality in the AC collagen network and/or its interactions with PG. This was an interesting finding as *in vitro* contact stress experiments would suggest that this region of the joint was under less loading following meniscectomy[44]. This leads us to speculate that, while this outer region was not under the high direct loading, as would be experienced by the central region of the tibia, it was still exposed to mediators of PG and collagen degradation originating from the inflammation of the synovium which also occurs in this model. In an earlier study using this animal model it was noted that the small dermatan sulfate containing PG, decorin, was lost from the lateral AC before degradation of aggrecan was evident[17]. Since decorin is known to interact strongly with type II collagen fibrils and has been shown to limit fibril assembly and aggregation, its depletion from the AC of the MEN joints could explain the enhancement of tissue swelling[45]. This hyper-hydration of AC would, as a consequence, lead to a disruption the thick type II collagen fibres of the superficial zone resulting in a disruption of their alignment. This hypothesis would explain the observed

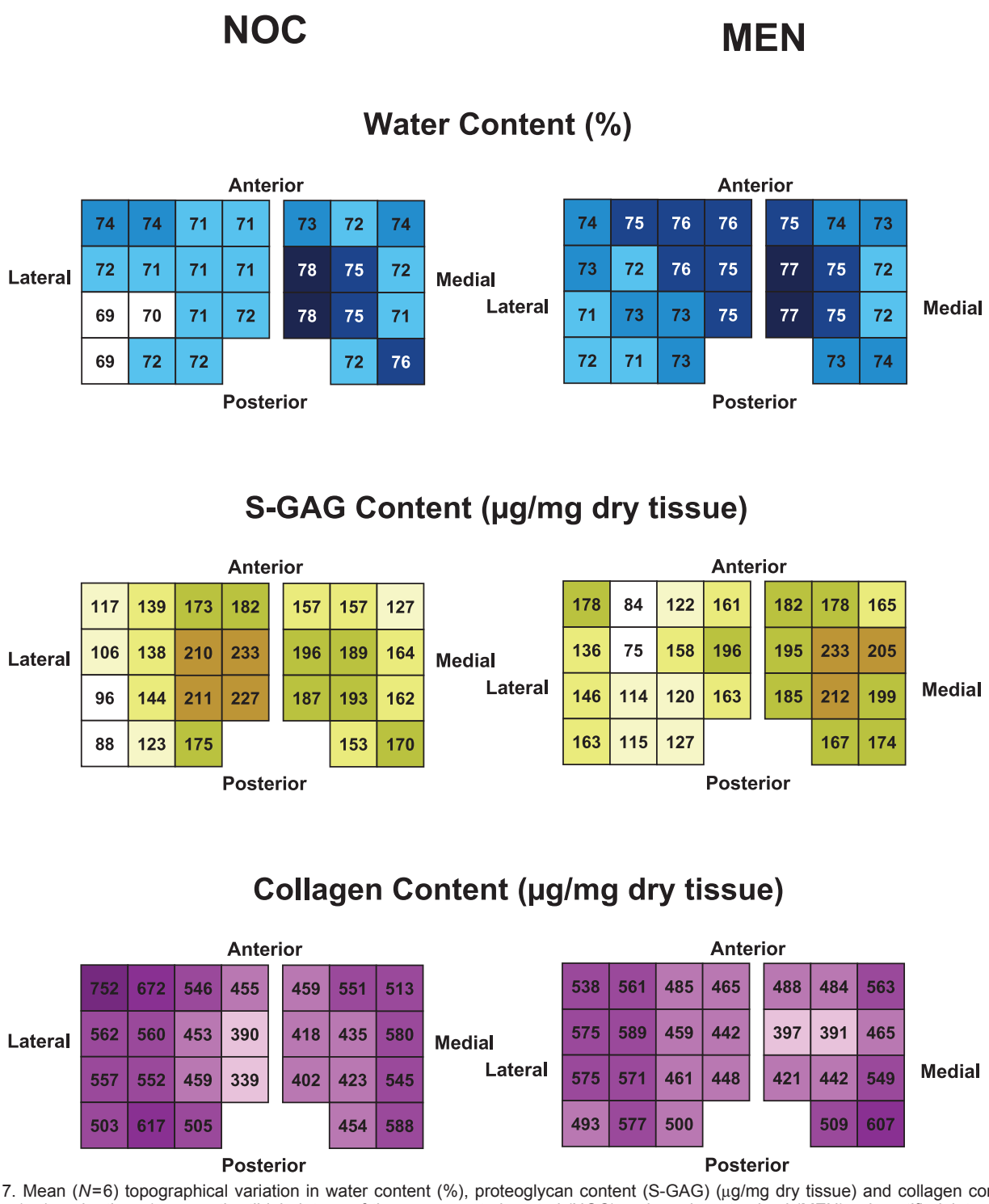

Fig. 7. Mean (N=6) topographical variation in water content (%), proteoglycan content (S-GAG) (µg/mg dry tissue) and collagen content (µg/mg dry tissue) across the tibial plateau of the non-operated control (NOC) and meniscectomized (MEN) ovine stifle joint.

changes in the birefringence profile in the outer region of AC from meniscectomized joints, particularly in the superficial zone. In addition, the reduction in collagen organization at the surface of AC would reduce its dynamic stiffness. It is noteworthy in this regard that the biochemical profile of the hypertrophic outer region, after meniscectomy, resembles the NOC inner region, which is normally in direct contact with the femoral condyle. Therefore, this early hypertrophic response following meniscectomy may reflect the reorganization of the collagen architecture. Another alternative to this explanation is that the observed hypertrophy was due to tissue swelling, which may have occurred above the collagen arcs and below the most superficial collagen. This may not be easily visible in the processed histological sections but is plausible because the resulting decrease in collagen birefringence would be due to separation of pre-existing collagen fibres and the subsequent loss of collagen organization. A model for this

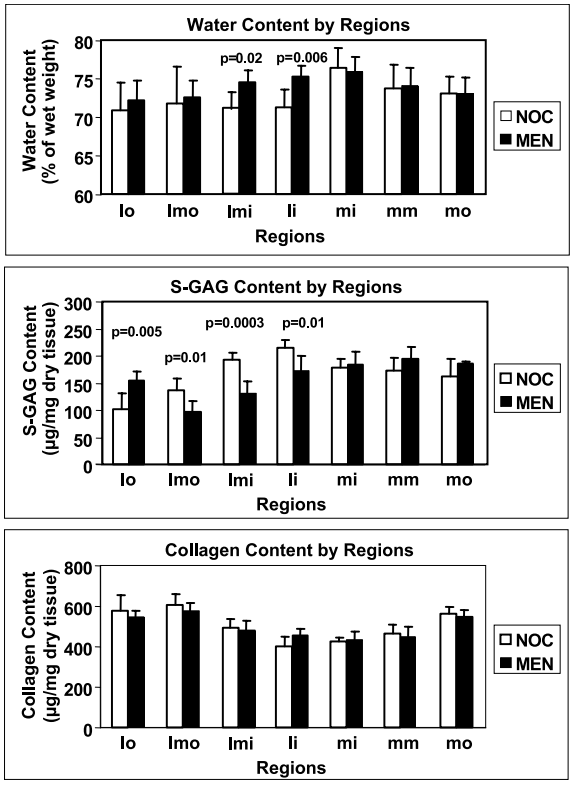

Fig. 8. Biochemical composition (water, S-GAG, and collagen content) of lateral and medial regions of tibial plateau articular cartilage of non-operated control (NOC) and meniscectomized (MEN) ovine stifle joints (N=6).

collagen re-organization arising during the hypertrophy response of AC in this model is shown in Fig. 10.

The articular cartilage of the medial–outer region also underwent some alterations following meniscectomy. These included an increase in AC thickness, and an increase in phase lag. We consider that these changes are a consequence of the altered kinematics of the joint resulting from the removal of the lateral meniscus, which causes an external rotation and lateral shift of the femoral condyles (Fig. 11). This not only increases the loading on the lateral compartment but also unloads the medial–outer region. In this regard it is noteworthy that a reduction in loading of AC is associated with its degeneration and decline of biomechanical properties[46]. Although not part of the present investigation, a gait analysis could provide additional information on the changed weight distribution, thereby supporting more direct correlations between the biomechanical and biochemical changes observed.

Using a canine medial meniscectomy model, followed over 3 months, LeRoux *et al.*[14] undertook similar biomechanical and biochemical studies to those described here. However, these authors reported no change in AC thickness or collagen birefringence in the joint sites they sampled. Meniscectomy of the canine stifle joint did induce a significant decrease in PG content, a 50% decrease in equilibrium compressive moduli, and lower dynamic shear moduli of AC, although only at low frequency (0.01 rad/s or 0.6 Hz). While LeRoux *et al.*[14] reported phase lag values for normal canine AC (12.9±3.1°), which were similar to those observed in our study, they found no change in phase lag of AC after meniscectomy. While this discrepancy may be explained by the different species used, it is more likely

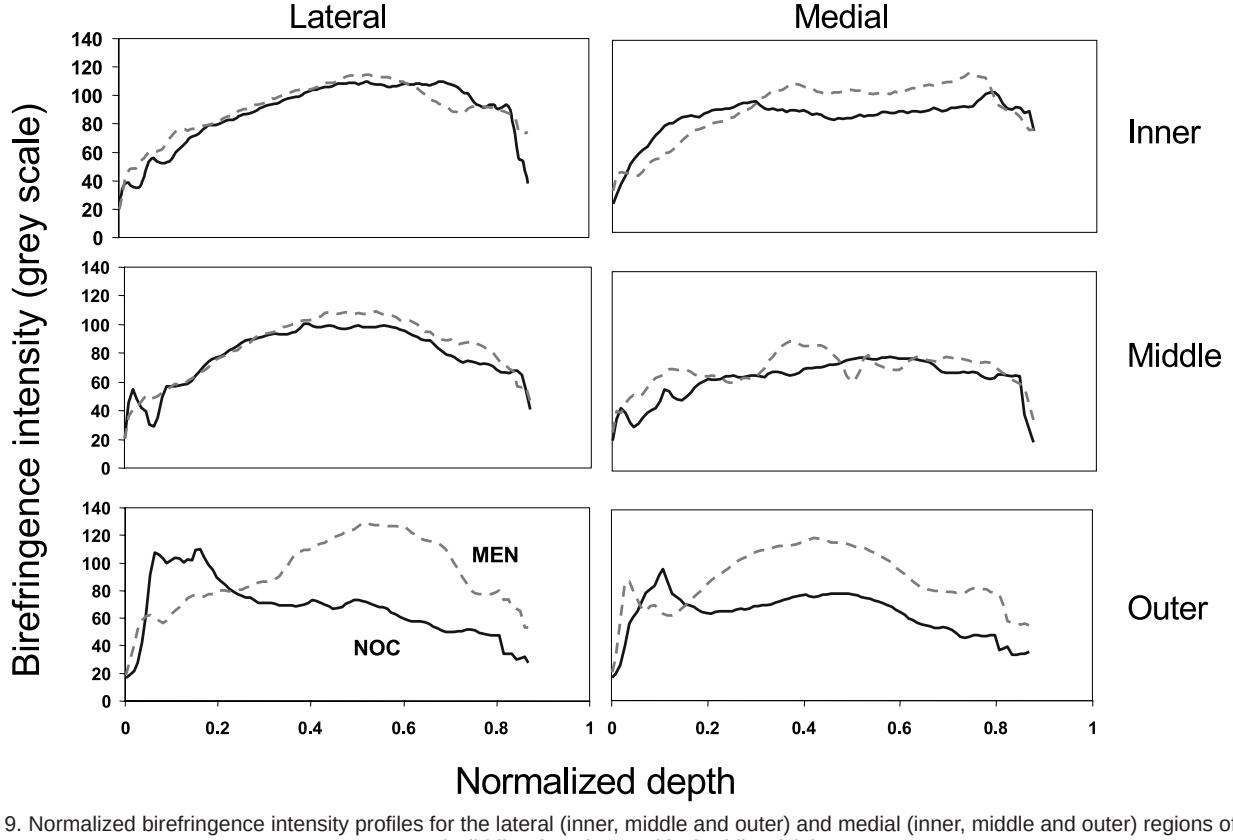

Fig. 9. Normalized birefringence intensity profiles for the lateral (inner, middle and outer) and medial (inner, middle and outer) regions of the NOC (solid lines) and MEN (dashed lines) joints.

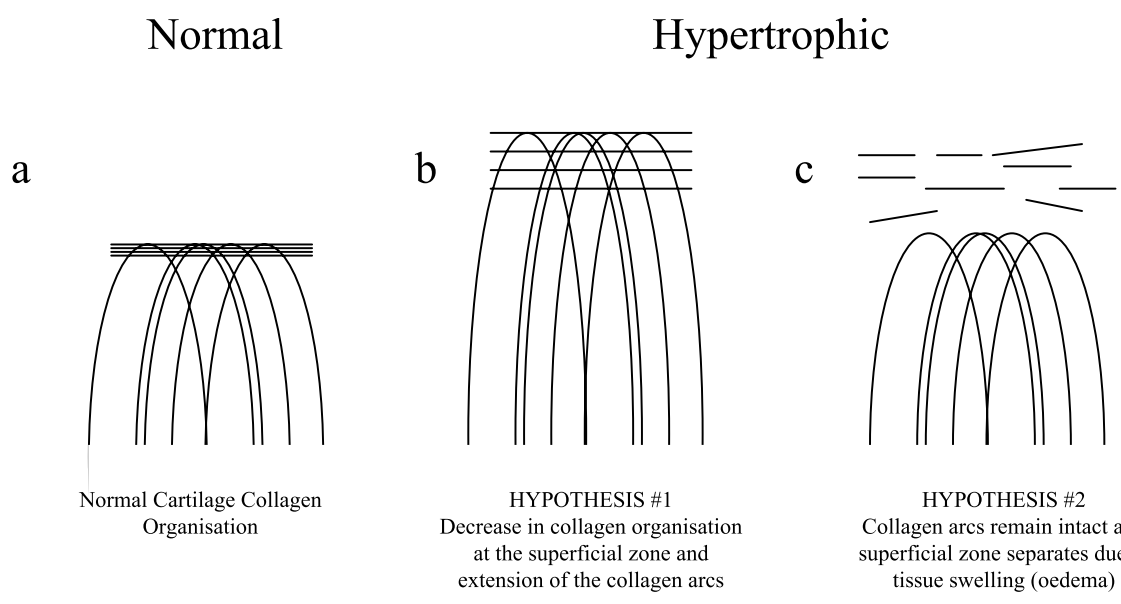

Fig. 10. Hypothesized alteration in collagen organization from normal (a) to hypertrophic cartilage (b) and (c). The superficial collagen of the hypertrophic tissue is either increasingly eroded, disorganized and the collagen arcs extended (b) or partly separated from the underlying arcs due to tissue swelling (oedema) in the transitional zone (c).

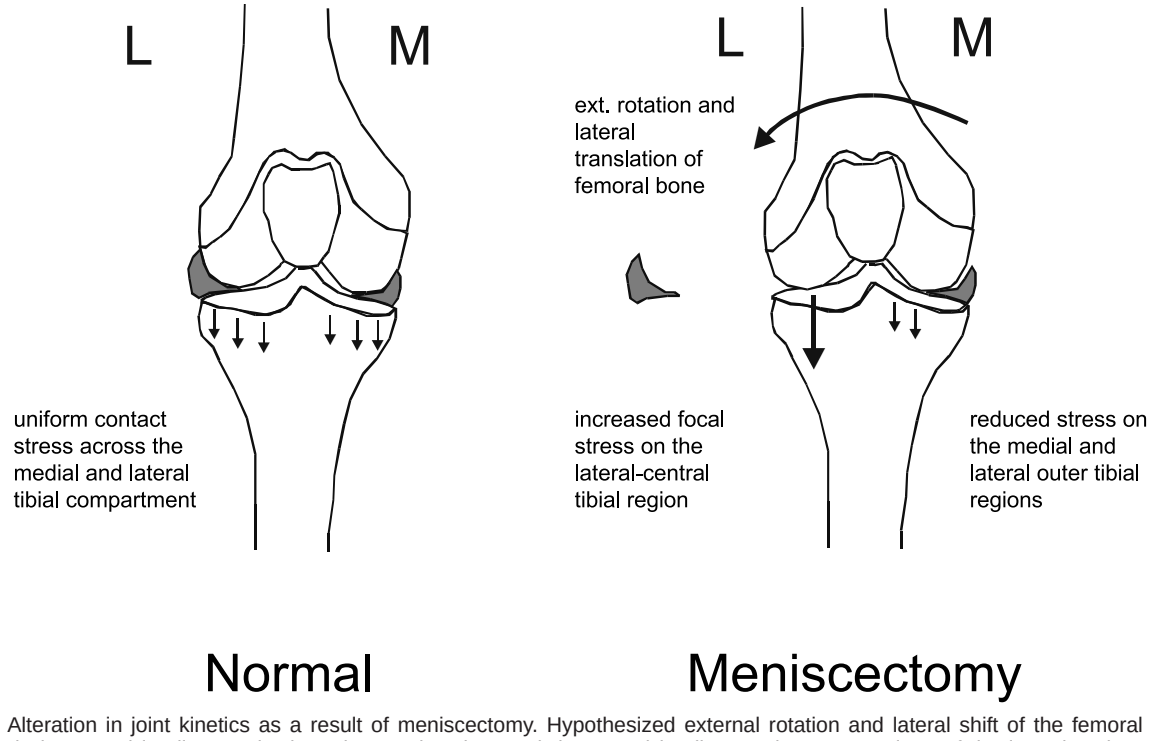

Fig. 11. Alteration in joint kinetics as a result of meniscectomy. Hypothesized external rotation and lateral shift of the femoral condyles resulting in increased loading on the lateral–central region, and decreased loading on the outer regions of the lateral and medial tibial compartments.

because our animals were (a) subjected to bilateral lateral meniscectomy, as opposed to unilateral medial meniscectomy and (b) weight bearing for an additional 3 months post-meniscectomy. Moreover, we undertook direct dynamic indentation of whole osteochondral sections of tibial plateaux as opposed to torsional loading of AC explants as used by LeRoux *et al.*[14].

The data generated by the present study has provided valuable information on the temporal and spatial changes which take place in knee joints following lateral meniscectomy, a procedure which is known to alter the distribution of mechanical stresses acting across joints. The results obtained have identified a spectrum of events, which, for the most part, reflect the response of the chondrocyte to altered mechanical stresses and highlights the inherent difficulties associated with defining the onset and development of OA in terms of cartilage composition and structure.

Acknowledgments

The authors thank Mrs Diana Pethick and Mr David Brockway of Murdoch University for their assistance with the animal handling and care. The expert contributions made by Mrs Susan Smith (histology) and Ms Lynne Campbell (manuscript) from the Institute of Bone and Joint Research are also gratefully acknowledged. The authors are grateful to one of the reviewers for the worthwhile comments and suggestion for the alternative model to explain our findings as illustrated in panel C of Fig. 10.

References

1. Roos H, Lauren M, Adalberth T, Roos EM, Jonsson K, Lohmander LS. Knee osteoarthritis after meniscectomy: prevalence of radiographic changes after twenty-one years, compared with matched controls. Arthritis Rheum 1998;41:687–93.
2. Jorgensen U, Sonne-Holm S, Lauridsen F, Rosenklint A. Long-term follow-up of meniscectomy in athletes. A prospective longitudinal study. J Bone Joint Surg [Br] 1987;69:80–3.
3. McNicholas MJ, Rowley DI, McGurty D, Adalberth T, Abdon P, Lindstrand A, *et al*. Total meniscectomy in adolescence. A thirty-year follow-up. J Bone Joint Surg Br 2000;82:217–21.
4. Markolf KL, Mensch JS, Amstutz HC. Stiffness and laxity of the knee—the contributions of the supporting structures. A quantitative *in vitro* study. J Bone Joint Surg Am 1976;58:583–94.
5. Seedhom BB, Hargreaves DJ. Transmission of the load in the knee joint with special reference to the role of the menisci. I. Anatomy, analysis and apparatus. Eng Med 1979;8:207–219.
6. Kurosawa H, Fukubayashi T, Nakajima H. Load-bearing mode of the knee joint: physical behavior of the knee joint with or without menisci. Clin Orthop 1980;00:283–90.
7. Voloshin AS, Wosk J. Shock absorption of meniscectomized and painful knees: a comparative in vivo study. J Biomed Eng 1983;5:157–61.
8. Allen CR, Wong EK, Livesay GA, Sakane M, Fu FH, Woo SL. Importance of the medial meniscus in the anterior cruciate ligament-deficient knee. J Orthop Res 2000;18:109–15.
9. Smith M, Ghosh P. Experimental models of osteoarthritis. In: Moskowitz RW, Howell DS, Altman RD, Buckwalter JA, Goldberg VM, Eds. Osteoarthritis. Diagnosis and Medical/Surgical Management. Philadelphia, London, New York, St. Louis, Sydney, Toronto: WB Saunders 2001:171–99.
10. Little C, Smith S, Ghosh P, Bellenger C. Histomorphological and immunohistochemical evaluation of joint changes in a model of osteoarthritis induced by lateral meniscectomy in sheep. J Rheumatol 1997;24:2199–209.
11. Bylski-Austrow DI, Malumed J, Meade T, Grood ES. Knee joint contact pressure decreases after chronic meniscectomy relative to the acutely meniscectomized joint: a mechanical study in the goat. J Orthop Res 1993;11:796–804.
12. Hoch DH, Grodzinsky AJ, Koob TJ, Albert ML, Eyre DR. Early changes in material properties of rabbit articular cartilage after meniscectomy. J Orthop Res 1983;1:4–12.
13. Elliott DM, Guilak F, Vail TP, Wang JY, Setton LA. Tensile properties of articular cartilage are altered by meniscectomy in a canine model of osteoarthritis. J Orthop Res 1999;17:503–8.
14. LeRoux MA, Arokoski J, Vail TP, Guilak F, Hyttinen MM, Kiviranta I, *et al*. Simultaneous changes in the mechanical properties, quantitative collagen organization, and proteoglycan concentration of articular cartilage following canine meniscectomy. J Orthop Res 2000;18:383–92.
15. Ghosh P, Numata Y, Smith S, Read R, Armstrong S, Johnson K. The metabolic response of articular cartilage to abnormal mechanical loading induced by medial or lateral meniscectomy. Agents Actions (Suppl) 1993;39:89–93.
16. Ghosh P, Read R, Numata Y, Smith S, Armstrong S, Wilson D. The effects of intra-articular administration of hyaluronan in a model of early osteoarthritis in sheep. II. Cartilage composition and proteoglycan metabolism. Semin Arthritis Rheum 1993;22:31–42.
17. Little CB, Ghosh P, Bellenger CR. Topographic variation in biglycan and decorin synthesis by articular cartilage in the early stages of osteoarthritis: An experimental study in sheep. J Orthop Res 1996;14:433–44.
18. Little CB, Ghosh P. Variation in proteoglycan metabolism by articular chondrocytes in different joint regions is determined by post-natal mechanical loading. Osteoarthritis Cart 1997;5:49–62.
19. Appleyard RC, Ghosh P, Swain MV. Biomechanical, histological and immunohistological studies of patellar cartilage in an ovine model of osteoarthritis induced by lateral meniscectomy. Osteoarthritis Cart 1999;7:281–94.
20. Burkhardt D, Hwa SY, Ghosh P. A novel microassay for the quantitation of the sulfated glycosaminoglycan content of histological sections: its application to determine the effects of Diacerhein on cartilage in an ovine model of osteoarthritis. Osteoarthritis Cart 2001;9:238–47.
21. Cake MA, Read RA, Guillou B, Ghosh P. Modification of articular cartilage and subchondral bone pathology in an ovine meniscectomy model of osteoarthritis by avocado and soya unsaponifiables (ASU). Osteoarthritis Cart 2000;8:404–11.
22. Hwa SY, Burkhardt D, Little C, Ghosh P. The effects of orally administered diacerein on cartilage and subchondral bone in an ovine model of osteoarthritis. J Rheumatol 2001;28:825–34.
23. Appleyard RC, Swain MV, Khanna S, Murrell GA. The accuracy and reliability of a novel handheld dynamic indentation probe for analysing articular cartilage. Phys Med Biol 2001;46:541–50.
24. Swann AC, Seedhom BB. Improved techniques for measuring the indentation and thickness of articular cartilage. Proc Inst Mech Eng H 1989;203:143–50.
25. Hayes WC, Keer LM, Herrmann G, Mockros LF. A mathematical analysis for indentation tests of articular cartilage. J Biomech 1972;5:541–51.
26. Lee RC, Frank EH, Grodzinsky AJ, Roylance DK. Oscillatory compressional behavior of articular cartilage and its associated electromechanical properties. J Biomech Eng 1981;103:280–92.
27. Appleyard RC, Swain MV, Ghosh P. Modification of the dynamic shear modulus and phase lag properties of tibial plateau articular cartilage in an ovine model of

osteoarthritis by oral administration of calcium pentosan polysulphate. Trans Orthop Res Soc 2000;320.
28. Farndale RW, Sayers CA, Barrett AJ. A direct spectrophotometric microassay for sulfated glycosaminoglycans in cartilage cultures. Connect Tissue Res 1982;9:247–8.
29. Stegemann H, Stalder K. Determination of hydroxyproline. Clin Chim Acta 1967;18:267–73.
30. Junqueira LC, Bignolas G, Brentani RR. Picrosirius staining plus polarization microscopy, a specific method for collagen detection in tissue sections. Histochem J 1979;11:447–55.
31. Arokoski JP, Hyttinen MM, Lapvetelainen T, Takács P, Kosztáczky B, Módis L, *et al*. Decreased birefringence of the superficial zone collagen network in the canine knee (stifle) articular cartilage after long distance running training, detected by quantitative polarised light microscopy. Ann Rheum Dis 1996;55: 253–64.
32. Setton LA, Mow VC, Howell DS. Mechanical behavior of articular cartilage in shear is altered by transection of the anterior cruciate ligament. J Orthop Res 1995;13:473–82.
33. Hardingham TE, Muir H, Kwan MK, Lai WM, Mow VC. Viscoelastic properties of proteoglycan solutions with varying proportions present as aggregates. J Orthop Res 1987;5:36–46.
34. Mow VC, Zhu W, Lai WM, Hardingham TE, Hughes C, Muir H. The influence of link protein stabilization on the viscometric properties of proteoglycan aggregate solutions. Biochim Biophys Acta 1989;992:201–8.
35. Hayes WC, Bodine AJ. Flow-independent viscoelastic properties of articular cartilage matrix. J Biomech 1978;11:407–19.
36. Bader DL, Kempson GE, Barrett AJ, Webb W. The effects of leucocyte elastase on the mechanical properties of adult human articular cartilage in tension. Biochim Biophys Acta 1981;677:103–8.
37. Bader DL, Kempson GE, Egan J, Gilbey W, Barrett AJ. The effects of selective matrix degradation on the short-term compressive properties of adult human articular cartilage. Biochim Biophys Acta 1992;1116: 147–54.
38. Parsons JR, Black J. Mechanical behavior of articular cartilage quantitative changes with enzymatic alteration of the proteoglycan fraction. Bull Hosp Jt Dis Orthop Inst 1987;47:13–30.
39. Jurvelin J, Säämänen AM, Arokoski J, Helminen HJ, Kiviranta I, Tammi M. Biomechanical properties of the canine knee articular cartilage as related to matrix proteoglycans and collagen. Eng Med 1988;17: 157–62.
40. Appleyard RC, Szomor ZL, Ghosh P, Swain MV, Murrell GAC. Loss of proteogylcans from articular cartilage increases dynamic phase lag but does not affect shear modulus: Application of a novel arthroscopic indentation device. Trans Orthop Res Soc 2002;48:396.
41. Zhu W, Iatridis JC, Hlibczuk V, Ratcliffe A, Mow VC. Determination of collagen–proteoglycan interactions in vitro. J Biomech 1996;29:773–83.
42. Zhu W, Mow VC, Koob TJ, Eyre DR. Viscoelastic shear properties of articular cartilage and the effects of glycosidase treatments. J Orthop Res 1993;11: 771–81.
43. Bank RA, Soudry M, Maroudas A, Mizrahi J, TeKoppele JM. The increased swelling and instantaneous deformation of osteoarthritic cartilage is highly correlated with collagen degradation. Arthritis Rheum 2000;43:2202–10.
44. Ahmed AM, Burke DL. In vitro measurement of static pressure distribution in synovial joints—Part I: Tibial surface of the knee. J Biomech Eng 1983;105: 216–25.
45. Roughley PJ, Lee ER. Cartilage proteoglycans: structure and potential functions. Microsc Res Tech 1994;28:385–97.
46. Jurvelin J, Kiviranta I, Tammi M, Helminen JH. Softening of canine articular cartilage after immobilization of the knee joint. Clin Orthop 1986;00:246–52.